Atmos. Meas. Tech., 7, 1245–1257, 2014
www.atmos-meas-tech.net/7/1245/2014/
doi:10.5194/amt-7-1245-2014

Atmospheric Measurement Techniques Open Access

Peroxy radical detection for airborne atmospheric measurements using absorption spectroscopy of NO_2

M. Horstjann, M. D. Andrés Hernández, V. Nenakhov, A. Chrobry, and J. P. Burrows

Institute of Environmental Physics, University of Bremen (IUP-UB), Otto-Hahn-Allee 1, 28359 Bremen, Germany

Correspondence to: M. Horstjann (markus.horstjann@iup.physik.uni-bremen.de)

Received: 18 September 2013 – Published in Atmos. Meas. Tech. Discuss.: 8 November 2013
Revised: 3 March 2014 – Accepted: 14 March 2014 – Published: 13 May 2014

Abstract. Development of an airborne instrument for the determination of peroxy radicals (PeRCEAS – peroxy radical chemical enhancement and absorption spectroscopy) is reported. Ambient peroxy radicals (HO_2 and RO_2, R being an organic chain) are converted to NO_2 in a reactor using a chain reaction involving NO and CO. Provided that the amplification factor, called effective chain length (eCL), is known, the concentration of NO_2 can be used as a proxy for the peroxy radical concentration in the sampled air. The eCL depends on radical surface losses and must thus be determined experimentally for each individual setup. NO_2 is detected by continuous-wave cavity ring-down spectroscopy (cw-CRDS) using an extended cavity diode laser (ECDL) at 408.9 nm. Optical feedback from a V-shaped resonator maximizes transmission and allows for a simple detector setup. CRDS directly yields absorption coefficients, thus providing NO_2 concentrations without additional calibration. The optimum 1σ detection limit is 0.3 ppbv at an averaging time of 40 s and an inlet pressure of 300 hPa. Effective chain lengths were determined for HO_2 and CH_3O_2 at different inlet pressures. The 1σ detection limit at an inlet pressure of 300 hPa for HO_2 is 3 pptv for an averaging time of 120 s.

1 Introduction

The hydroperoxy radical (HO_2) and organic peroxy radicals (RO_2, R being an organic chain), hereafter referred to as peroxy radicals, are known for their importance in photochemical reaction cycles both in the stratosphere (Thrush et al., 1998) and troposphere (Monks, 2005). They are very reactive species, and in combination with the hydroxyl radical (OH) play a crucial role in most atmospheric oxidation mechanisms which lead to the formation of O_3, peroxyacetyl nitrate (PAN, see Table A1 – list of acronyms), aldehydes and acids. To fully characterize the photochemical activity of the atmosphere, it is therefore highly desirable to include peroxy radical concentrations. Furthermore, for certain environments modeled and measured concentrations disagree to a significant amount, pointing towards a yet unknown radical recycling process (Lelieveld et al., 2008; Hofzumahaus et al., 2009; Whalley et al., 2011). Although their ambient concentrations are generally low, peak mixing ratios of up to 100 pptv have been observed (Burkert et al., 2001a; Hofzumahaus et al., 2009).

The direct measurement of peroxy radicals remains a challenging task due to their high reactivity and thus short lifetime. The only existing technique for direct and speciated measurements is the matrix isolation electron spin resonance (MIESR) Spectroscopy, which traps them in a LN_2-cooled D_2O matrix. The required long sampling times of ~ 30 min and the offline analysis in the laboratory by probing their rotational transitions are important limitations of this technique (Mihelcic et al., 1985; Fuchs et al., 2009). Recent direct HO_2 detection setups by Djehiche et al. (2011), and Bell et al. (2012), employing cavity ring-down spectroscopy (CRDS) and noise-immune cavity enhanced optical heterodyne molecular spectroscopy (NICE-OHMS), respectively, still lack the necessary sensitivity for ambient measurements.

Other techniques like laser-induced fluorescence (LIF), chemical ionization mass spectrometry (CIMS), and peroxy radical chemical amplification (PeRCA) are used for the indirect measurement of peroxy radicals. All of them have been deployed for airborne measurements as described in more detail in Heard (2006).

The PeRCA technique determines the sum of peroxy radicals $[RO_2^*]$ ($:=[HO_2]+\sum[RO_2]$) by facilitating a chain reaction of peroxy radicals into the less reactive species NO_2, whose concentration is then measured (Cantrell and Stedman, 1982; Cantrell et al., 1984; Hastie et al., 1991).

The chemical conversion of peroxy radicals to NO_2 is achieved by adding NO and CO to the sample air in a reactor, thus enabling the reactions

$$HO_2 + NO \rightarrow OH + NO_2 \quad \text{(R1)}$$

and

$$OH + CO + O_2 + M \rightarrow HO_2 + CO_2 + M. \quad \text{(R2)}$$

The HO_2 radical is thus recycled, initiating the chain reaction.

Similarly, ambient RO_2 radicals are contributing to the NO_2 concentration by

$$RO_2 + NO \rightarrow RO + NO_2, \quad \text{(R3)}$$

before also taking part in the chain reaction via HO_2

$$RO + O_2 \rightarrow HO_2 + \text{aldehydes/carbonyl compounds}. \quad \text{(R4)}$$

Thus, both HO_2 and RO_2 convert NO to NO_2 via the chain reaction involving HO_2. The contribution of ambient OH and RO radicals to the production of NO_2 in the reactor can be neglected due to their comparably low abundance in the atmosphere. Note that the efficiency for RO_2 conversion is affected by additional terminating reactions depending on their chemical complexity.

The chain reaction increases the sensitivity to peroxy radicals as the number of molecules to measure is multiplied by the length of the chain reaction, the so-called chain length (CL). This CL depends on a series of terminating reactions and physical losses limiting the amplification in the reactor, which have been described in detail elsewhere (Hastie et al., 1991; Clemitshaw et al., 1997; Cantrell et al., 1993; Reichert et al., 2003). The concentration of the added gases (CO and NO) and both the reactor shape and its material are critical for the efficiency of those terminating processes. The total conversion into NO_2 is additionally affected by any other radical losses of the sampled air before it reaches the reactor where the amplification takes place. These can specially be enhanced by air-surface contacts in a pressure-regulated inlet. The total amplification factor, being called effective chain length (eCL), must therefore be determined experimentally for each particular setup. The eCL can be determined by sampling known peroxy radical mixtures under controlled conditions. Note that $eCL \leq CL$ as the measured multiplier eCL incorporates radical losses due to the air-surface contact. Chain length calibrations of HO_2 and CH_3O_2 are appropriate for airborne measurements where these two peroxy radicals are expected to dominate.

For the determination of the peroxy radical concentrations, the PeRCA technique usually operates alternatingly between a so-called "amplification mode" (CO is added, so the chain reaction takes place) and a "background mode" (where CO is replaced with N_2, suppressing the chain reaction). The background concentration $[NO_2]_{ambient}$ is enhanced both by species reacting with NO (e.g., ozone) or by being (thermally) decomposed in the inlet (e.g., PAN). This contribution is denoted by $[NO_2]_{other}$. Note that peroxy radicals themselves also contribute to this background through their direct reaction with NO. However, their atmospheric abundance is generally lower than 100 pptv, thus their contribution is considered to be negligible as the background is dominated by ambient O_3 in the ppbv range.

The resulting $[NO_2]_{meas}$ concentration measured is thus composed of

$$[NO_2]_{meas} = [NO_2]_{ambient} + [NO_2]_{other} + eCL \times \left[RO_2^*\right], \quad (1)$$

where

$$\left[RO_2^*\right] := [HO_2] + \sum[RO_2], \quad (2)$$

neglecting both OH and $\sum$RO. The background mode thus only measures the first two addends of Eq. (1), and the difference in the NO_2 concentration between amplification and background mode constitutes the peroxy radical mediated part. Thus

$$\Delta[NO_2] := [NO_2]_{ampl} - [NO_2]_{backgr} = eCL \times \left[RO_2^*\right]. \quad (3)$$

The PeRCA technique has been complemented by, for example, Chemiluminescence, LIF (Sadanaga et al., 2004), or cavity ring-down spectroscopy (CRDS) for the detection of NO_2 (Heard, 2006). A highly sensitive chemical method using chemiluminescence detection is the reaction of NO_2 with a luminol (3-aminophthalhydrazide: $C_8H_7N_3O_2$) solution (Maeda et al., 1980). This yields excellent (3σ) detection limits for the total sum of peroxy radicals of 3 ± 2 pptv ($eCL = 45 \pm 7$, pressure 200 hPa, averaging time 20 s, Kartal et al., 2010) and it has been used in numerous measurement campaigns, both ground-based (Cantrell et al., 1993; Clemitshaw et al., 1997; Burkert et al., 2001b; Andrés Hernández et al., 2001; Fleming et al., 2006; Andrés-Hernández et al., 2013) and airborne (Green et al., 2002; Andrés Hernández et al., 2010; Kartal et al., 2010). Although well established for airborne measurements, the luminol detector still presents some drawbacks, like its range of linearity and the dependency of the sensitivity to humidity and pressure (Wendisch and Brenguier, 2013). In order to overcome these limitations the PeRCEAS instrument was developed at the Institute of Environmental Physics, which employs a variant of laser absorption spectroscopy called CRDS to measure the NO_2 concentration. A V-shaped optical resonator provides optical feedback to the employed extended cavity diode laser (ECDL), stabilizing the laser emission

wavelength and enhancing resonator transmission. The use of an optical method to detect NO_2 presents some clear advantages. Optical detection of NO_2 is chemically specific, does not require a constant addition of NO_2 to assure detector signal linearity, and is not affected by NO which is added to the sampled air. These benefits provide greater freedom in selecting measurement conditions maximizing conversion and amplification parameters (e.g., increasing NO mixing ratios in the reactor for improving the chemical conversion without deteriorating detection sensitivity). Furthermore, the decrease of the sensitivity of the luminol detection at lower pressures limits its use for measurements in the upper layers of the troposphere.

A similar configuration using the PeRCA technique and a CRDS NO_2 detector (albeit without optical feedback) is described in Liu et al. (2009), who reported on an instrument for ground-based measurements at standard pressure. It is a combination of a NO_2 CRDS detector (Hargrove et al., 2006) and a 5 m-long (Teflon) tubing system enabling the peroxy radical chemical conversion. Its eCL is calibrated using rather high amounts (compared to typical atmospheric abundances) of HO_2 between 0.5 and 3 ppbv generated by thermal decomposition of H_2O_2 (see Sect. 3.2 for the PeRCEAS chain length calibration). Investigation of the dependency of the eCL on ambient air humidity is not mentioned. The NO_2 detector employs a Nd-YAG pumped dye laser and a resonator incorporating mirrors with a distance of 1 m (see Sect. 2.2 for the PeRCEAS NO_2 detector description).

CRDS is a technique well known for its sensitivity and robustness. Already employed in 1988 for absorption measurements (O'Keefe and Deacon, 1988), it is nowadays one of the dominant trace gas absorption measurement techniques. Reviews of this spectroscopy method may be found in Busch and Busch (1999), or, more recently, in Berden and Engeln (2010). Briefly, a resonator consisting of highly reflective mirrors is filled with the sample air to be measured. Usually a laser is used for resonator excitation, and if an operator-set resonator transmission intensity is reached, the laser is switched off rapidly. The subsequent decay of this transmission yields the ring-down time τ after which the intensity has decayed to e^{-1} of its initial value. The losses leading to this decay incorporate absorption and scattering both from the mirrors themselves and from the sample air. The absorption coefficient α of an absorber of interest can be calculated directly from two ring-down time measurements; one with the sample air inside the resonator not containing the absorber (yielding τ_0, which also incorporates the mirror reflectivity) and one with the absorber present (yielding τ_α):

$$\alpha = \frac{n}{c_0} \times \left(\frac{1}{\tau_a} - \frac{1}{\tau_0} \right), \tag{4}$$

where n is the index of refraction (here: of the sample air), and c_0 is the speed of light in vacuum.

The absorber concentration $\frac{N}{V}$ can then be calculated using

$$\alpha = \frac{N}{V} \times \sigma^{\lambda}_{\text{absorber}}, \tag{5}$$

where N is the number of molecules, V is the volume, and $\sigma^{\lambda}_{\text{absorber}}$ is the absorption cross section at the laser wavelength λ. Here, the absorber is NO_2 and $\sigma^{408.9\text{nm}}_{NO_2} = 6.5 \times 10^{-19}\,\text{cm}^2\,\text{molecule}^{-1}$ is the absorption cross section at the laser wavelength of 408.9 nm, a temperature of 296 K and a pressure of 300 hPa (Vandaele et al., 2002; Nizkorodov et al., 2004). This value was experimentally verified to ±2 % by flowing synthetic air with different NO_2 concentrations through the resonator and measuring the corresponding ring-down times (see Sect. 3.1). To determine the peroxy radical concentration, the NO_2 concentration difference between background and amplification modes is required. Thus, ring-down measurements taken during the background yield τ_0 and those taken during the amplification mode yield τ_α in Eq. (4).

2 Experimental

Figure 1 shows the schematic setup of the PeRCEAS instrument developed for operation on the research aircraft HALO (high altitude and long range research aircraft – see http://www.halo.dlr.de/ for further information). The PeRCEAS instrument can be divided in two main parts; one is the inlet (outer dimension 73 cm × 32 cm × 24 cm; total weight 21 kg), which is installed in the aircraft fuselage to sample the outside air, and the other is the NO_2 detectors analyzing the sampled (and chemically converted) air. The sampled air proceeds either through a bypass, which is used for the inlet pressure regulation, or to the reactors and NO_2 detectors to be measured. The latter air is then scrubbed of NO_x and CO before being merged with the bypass flow again. The NO_2 detectors are mounted in a customized HALO 19″ rack (outer dimension 170 cm × 65 cm × 55 cm; mounted total weight 140 kg), which also contains the HALO power supply distribution, a 15″ monitor (VISAM GmbH), a local power distribution unit (Stachl Elektronik GmbH), the laser power supply, a DAQ (data acquisition) PXI computer (National Instruments), two Peltier temperature controllers (type MPT 10000, Wavelength Electronics) and one pressure and nine mass flow controllers (Bronkhorst Mättig GmbH). The rack bottom also contains a drawer which houses a 600 ppmv NO in N_2 – and a 10 ppmv NO_2 in synthetic air gas cylinder and the corresponding pressure reducers. The NO_2 is to be used to seed outside air for a reference measurement if the measurement data indicates unusual instrument operation, for example, strongly degraded background ring-down times. Figure 2 shows the assembled PeRCEAS rack.

Additionally required components are a pure CO and a N_2 gas cylinder, a NO_x and a CO scrubber, and a vacuum

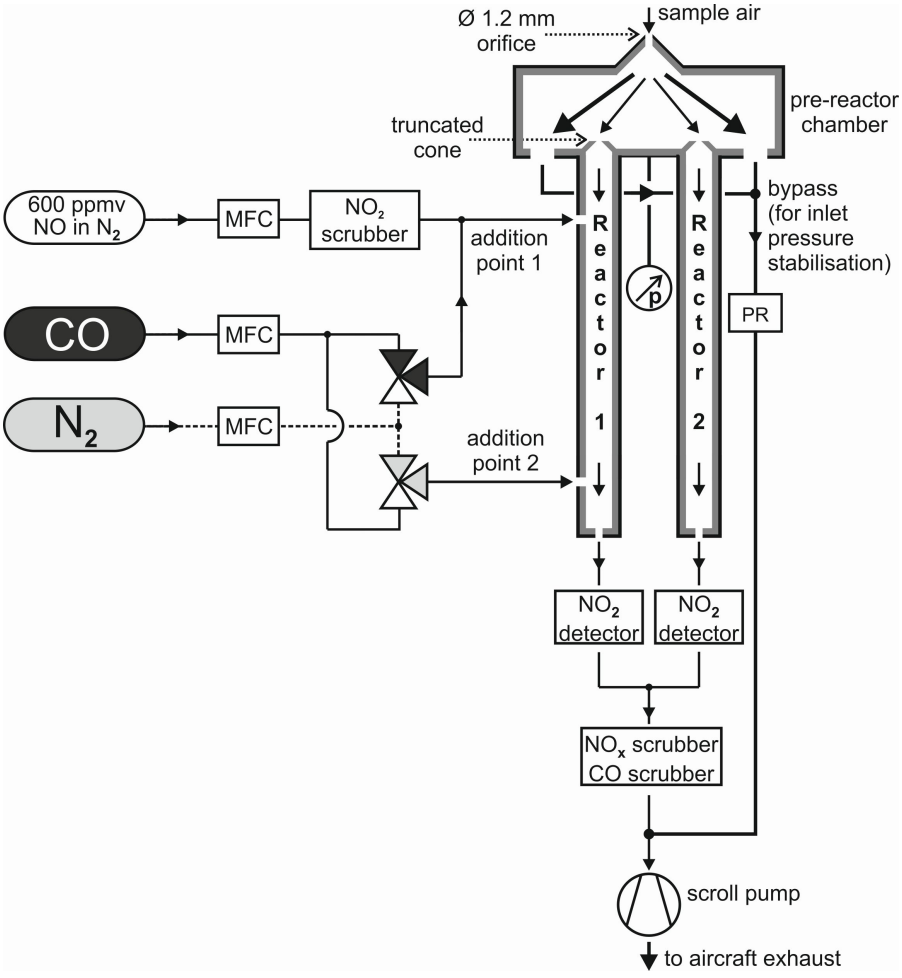

Fig. 1. Pressure and gas flow of the PeRCEAS instrument. Reactor 1 is shown in amplification mode. MFC – mass flow controller, PR – pressure regulator. The sensor between both reactors measures the inlet pressure. The ovals on the left side represent gas cylinders.

pump (Scrollvac SC 30 D, Oerlikon Leybold Vakuum). For safety reasons, the CO gas cylinder is placed in a specially designed containment. The whole system including the inlet has a weight of 250 kg.

2.1 Inlet

To avoid certification costs for a nonstandard gas inlet, the size and shape of the PeRCEAS inlet were designed to fit inside a HALO outer protection pylon for standard trace gas inlets. Figure 3 shows a photograph of the PeRCEAS inlet. It was developed based on previous experience with a DUALER (dual channel chemical amplifier – Kartal et al., 2010; Chrobry, 2013). The inlet is made of Teflon-coated stainless steel and consists of a pressure-controlled pre-reactor chamber (volume $\sim 100\,cm^3$), into which the sample air is sucked through a cone with a 1.2 mm orifice at its top, and two complete reactor-detector sampling lines running in parallel. Inside the reactors (inner diameter 17 mm, length 500 mm, volume $\sim 110\,cm^3$) the amplified conversion of peroxy radicals to NO_2 takes place. They are directly connected to the two CRDS NO_2 detectors via 1/4″ outer diameter black PFA tubing. The availability of two parallel sampling lines increase the instrument's reliability and allows continuous monitoring of the NO_2 background and its short-term variations.

The PeRCEAS pre-reactor chamber pressure is stabilized using a pressure sensor (type DMP 331, BD Sensors GmbH)/pressure regulator (Bronkhorst Mättig GmbH) combo. Two transparent 1/2″ outer diameter PFA connections on both sides of the pre-reactor chamber allow for the removal of the surplus air by the pressure regulator. Inlet pressure stabilization maintains a constant peroxy radical conversion time and thus eliminates the eCL dependence on the ambient pressure. In the lower troposphere it also significantly reduces the relative humidity and thus the humidity-dependent eCL variation (Kartal et al., 2010).

The optimum inlet pressure seeks to enable the measurement at high altitudes with suitable stability and sensitivity.

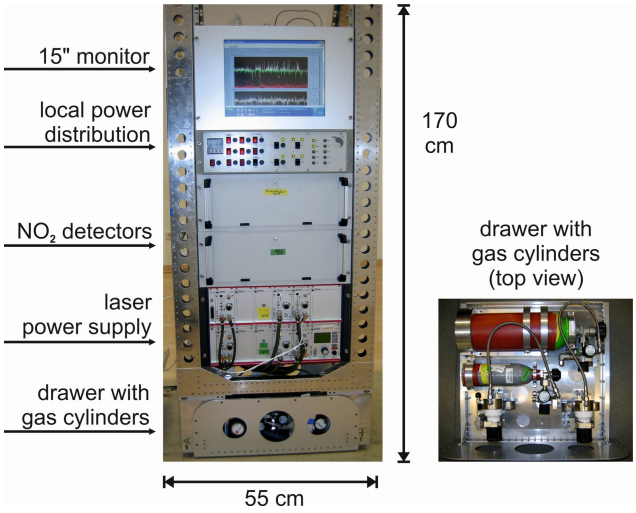

Fig. 2. PeRCEAS rack front side. Rack components which are not visible: PXI computer, temperature-, pressure- and flow controllers, and HALO power supply unit.

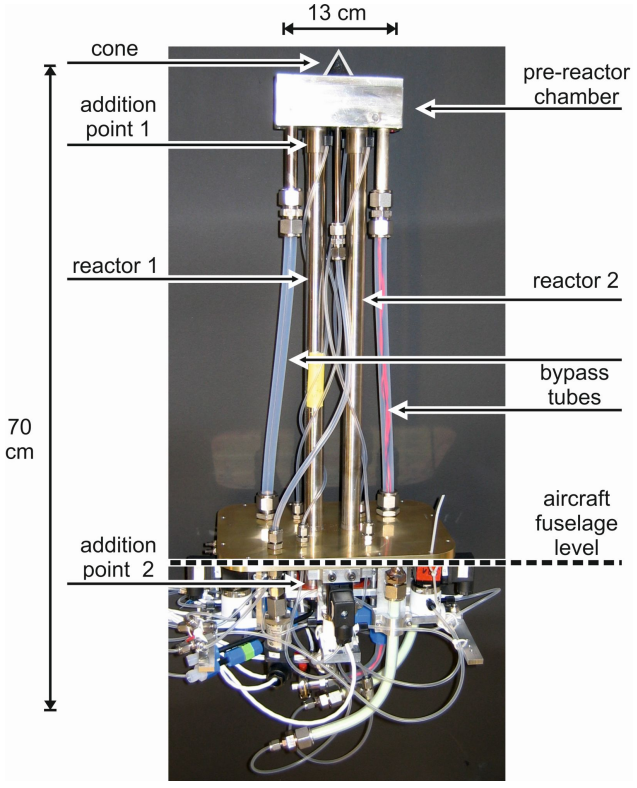

Fig. 3. Side view of the PeRCEAS inlet. Not shown: outer aircraft protection pylon and inner aircraft protection casing.

Very low pressures at the inlet imply however a deterioration in the eCL and the overall measurement stability. Therefore, an approach as shown in Fig. 4 is proposed. For altitudes below 8 km, the gas flow and pressure controlling is robust at a set inlet pressure of 300 hPa, leading to eCL values of around 100 (see Sect. 3.2 for a complete discussion) with a moderate time response of 15 s. For altitudes between 8 and 10 km an inlet pressure of 200 hPa yields a lower eCL of around 55 with a faster time response of 10 s, whereas at higher altitudes the set inlet pressure of 100 hPa retains these 10 s, as only half of the sample flow can be achieved by the actual setup under these conditions.

During the amplification mode a mixture of 0.09 sLpm pure CO and 0.01 sLpm 600 ppmv NO in N_2 is added to the sampled air at the reactor top (addition point 1, Fig. 3), whereas 0.09 sLpm N_2 is added at the reactor bottom (addition point 2). In the background mode, the CO and N_2 addition is exchanged (N_2 and NO addition at the reactor top, CO at the reactor bottom). The total reactor flow of 1 sLpm and the mixing ratios of the added gases remain constant during the measurement (81 % vol sample air, 9 % vol CO, $\sim$ 10 % vol N_2, and 6 ppmv NO). The CO mixing ratio of 9 % vol ensures a high chain length but is still well below the 12 % vol mixing ratio that poses the danger of creating explosive mixtures. The rerouting of the added gases between the addition points is facilitated by Teflon three-way solenoid valves (type QE 622, Staiger GmbH). The NO gas is scrubbed by $FeSO_4$, removing non-negligible traces of NO_2, before being added to the gas stream of the reactor top.

To ensure a thorough mixing of the sample air with the added gases, the latter are distributed by eight circularly arranged Ø 1.5 mm orifices into the reactor. The cylindrical reactors end at the top in a truncated cone (4 mm top diameter, 14.2 mm height) protruding into the pre-reactor chamber. The shape and dimensions of these reactor inlets have been selected to prevent diffusion of the added gases into the pre-reactor chamber while minimizing the radical wall losses.

The PeRCEAS inlet was characterized regarding its operating conditions at an inlet pressure of 300 hPa utilizing a luminol chemiluminescence NO_2 detector (Chrobry, 2013). It was found that a Teflon-coated interior of both the pre-reactor chamber and the reactor doubles the eCL, emphasizing the importance of the choice of material to avoid radical wall losses.

2.2 NO_2 detector

The NO_2 detectors in their current stage stem from research on optical feedback cavity-enhanced absorption spectroscopy (OF-CEAS), as reported in Morville et al. (2005), and Courtillot et al. (2006). Briefly, a V-shaped resonator consisting of three highly reflective mirrors is excited via a wavelength-scanning continuous-wave laser. Optical feedback from the resonator forces the laser to stabilize itself onto a resonance frequency, yielding broad transmission lines. Resonator optical losses can be calculated from these transmissions if their maxima are calibrated with a ring-down time measurement. OF-CEAS thus outputs absorption spectra with a wavelength resolution governed by the resonator's

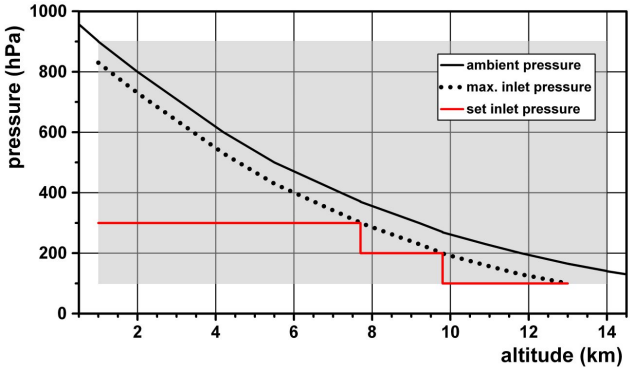

Fig. 4. Operating range of HALO aircraft measurements (shaded area). Maximum inlet pressure is assumed to be always 70 hPa lower than ambient pressure. The proposed set inlet pressure is shown in red. For an inlet pressure of 100 hPa the reactor flow must be reduced from 1 to 0.5 sLpm.

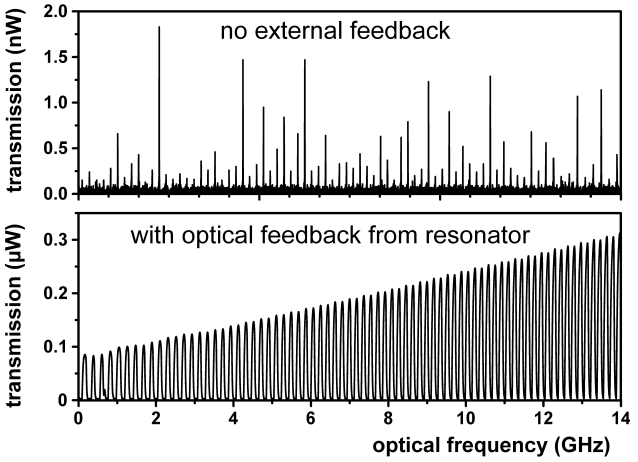

Fig. 5. Resonator transmission vs. relative laser frequency (at a wavelength of 408.9 nm) during a piezo scan (14 GHz = 7.8 pm at 408.9 nm) of the laser grating (Horstjann et al., 2012). Freely running ECDL (top panel); with the optical feedback from the high-finesse V-resonator (bottom panel). The signal slope is due to higher laser power at the end of the wavelength scan.

free spectral range. For an optimum configuration the distance between laser and resonator must be stabilized (usually by a mirror mounted on a piezo stack) using the symmetry of the transmission lines as an error signal.

The effect of optical feedback was characterized (Horstjann et al., 2012), and resonator transmissions with and without it during a laser scan can be seen in Fig. 5. The laser linewidth decreases about three orders of magnitude, and is temporarily locked to the resonator, yielding high resonator transmission (up to 1 % of the input power) which can be captured by a common Si photodiode detector.

The NO_2 detection limit for the detector using the OF-CEAS technique was determined to be $\sim$ 4 ppbv for 1 s averages and a resonator pressure of 290 hPa. For the detection of NO_2 in an aircraft environment, the OF-CEAS detection scheme proved to be too susceptible to both temperature variation and vibration, therefore the more robust technique of cavity ring-down spectroscopy (CRDS) was implemented. The continued use of the V-resonator allows the optical feedback to still provide high resonator transmission and bypasses the need for an optical isolator between laser and resonator.

The setup of the detector is shown schematically in Fig. 6 while Fig. 7 shows a photo of the 19″ case containing the ECD Laser (type DL-100L, wavelength 408.9 nm, max. 13 mW output power, 20 GHz modehop free tuning range, Toptica Photonics AG), the Si photodiode detector (type HCA-S, bandwidth 2 MHz, gain 5×10^5 VA^{-1}, Femto Messtechnik GmbH), a DAQ connection board, a power supply distribution board, a piezo stabilizing circuit (Floralis, France) and a fast TTL switch-off signal generator (Stachl Elektronik GmbH), cables, and gas flow components. The optical detector consists of an aluminium cuboid with a recess, forming a cavity. All optical components are fixed onto this cuboid; in other words, a $\lambda/2$ plate/polarization beam splitter combo (to adjust the optical feedback level), a prism on a manual linear stage (coarse adjustment of the laser-resonator distance), a mirror mounted onto a piezo stack (type P885.10, PI Ceramic GmbH) for fine adjustment of the laser-resonator distance, and the photodiode detector. The cuboid is mechanically isolated from the 19″ chassis by steel springs, and temperature isolated through 2 mm-thick aluminium sheets covered with Armaflex AF isolation material (Armacell Enterprise GmbH). Its temperature is also actively stabilized by a Peltier element (type CP-031, Te Technology Inc.). The sample air flow enters in the cuboid center and exits on both ends through NPT-threaded connections, and its temperature, pressure and relative humidity are measured. No aerosol or other gas filtering is used, and no adverse effects from mirror exposure to ambient air was experienced. At an inlet pressure of 300 hPa, the retention time of the sample air inside the resonator is $\sim$ 5 s.

The V-resonator is formed by a recess in the cuboid (volume $\sim$ 300 cm^3), sealed on top by a glued-in lid and on its sides by the glued-in highly reflective mirrors (diameter 1/2″, roc 100 cm, AT Films, USA). The lid itself contains small plates sealed with o-rings, which can be opened to clean the mirrors. The mirror-to-mirror distance is 40 cm, and the measured vacuum peak ring-down times of $\sim$ 26 µs yield an average mirror reflectivity of 99.995 % and a maximum light path of $\sim$ 8 km. For a resonator pressure of 285 hPa, the ring-down time is $\sim$ 20 µs and the light path thus $\sim$ 6 km. The laser is wavelength-scanned over $\sim$ 5 pm (about 10 GHz), generating $\sim$ 50 ring-down times per second. Each ring-down event is sampled for 300 µs. The ring-down times garnered in the amplification and background modes directly yield the absorption coefficient of the NO_2 that was formed by the peroxy radical chemical conversion. Changing

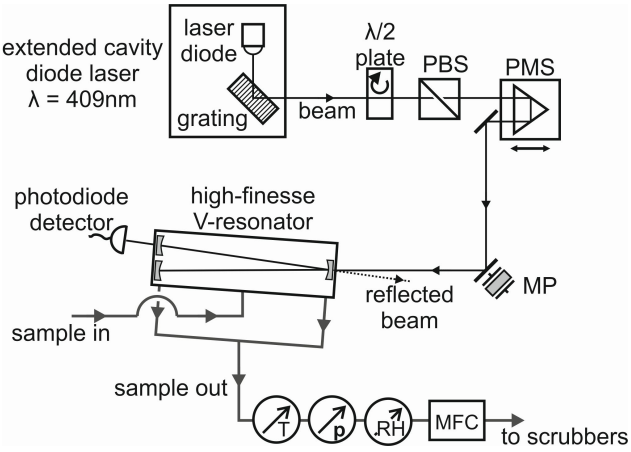

Fig. 6. Schematic diagram of a PeRCEAS NO_2 detector. PBS – polarizing beamsplitter, PMS – prism with micrometer screw, MP – mirror with piezo, MFC – mass flow controller. The sensors shown measure the temperature (T), pressure (p) and relative humidity (RH) of the sample gas. The use of the V-resonator allows for optical feedback, providing high transmission and obviating the need of an optical isolator between laser and resonator.

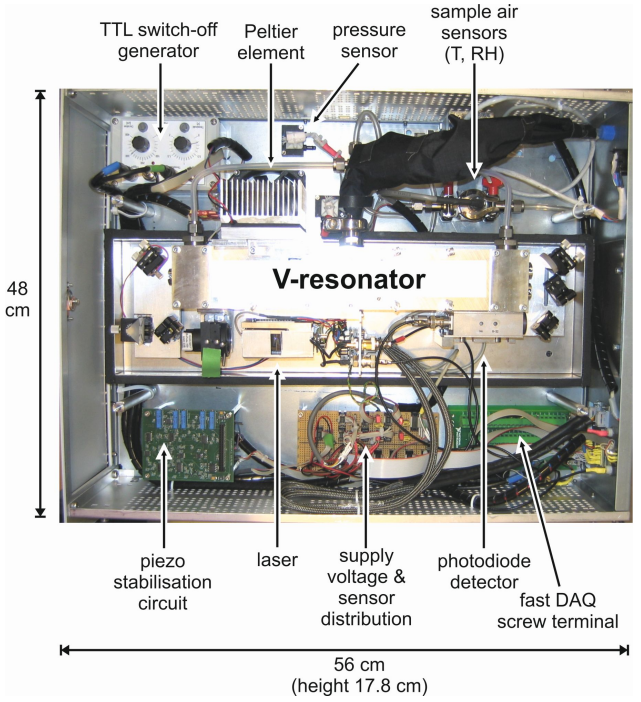

Fig. 7. Top view of the PeRCEAS NO_2 detector. The detector fits inside a 18 cm-high 19″ case whose front (here: left-hand side) can be opened. All electrical and gas connections are on its rear panel (here: right-hand side).

background concentrations of substances contributing to the NO_2 background are thus automatically accounted for if the change is slow compared to the duration of one background/amplification mode measurement (60 s in the present work).

The detector exhaust flows are purified by an activated charcoal scrubber removing the NO_x traces and a Pt/Al pellets scrubber converting CO to CO_2 at temperatures $T > 195\,°C$ before being merged with the inlet bypass flow (Fig. 1). The laser is scanned over 10 GHz at a wavelength of 408.9 nm, and if an operator-set resonator transmission intensity is reached, a fast ($< 1\,\mu s$) TTL signal is generated and fed to a FET circuit in parallel to the laser diode which then bypasses the laser diode, effectively switching off the laser. The ring-down signal is then sampled with (1 MSample) s^{-1} by a PXI-DAQ card (type PXI-6132, National Instruments), saved and analyzed with a PXI-computer (PXI-8105) by a custom LabVIEW program performing non-linear least-squares fits (Levenberg–Marquardt algorithm). The software provides 1 s-averaged ring-down values for online monitoring. Pressure-, flow-, temperature- and humidity sensor data are sampled at (1 Sample) s^{-1} (PXI-6129) and shown also by the LabVIEW program.

3 Results and discussion

Accurate calculation of peroxy radical mixing ratios demands the knowledge of both the eCL and the NO_2 mixing ratio difference Δx_{NO_2} introduced by the peroxy radical conversion. The latter is straightforward as the CRDS technique yields absorption coefficients that translate into concentrations if the absorption cross section σ_{NO_2} is known. Volume mixing ratios can then be calculated with the temperature and pressure of the sample air. The detector sensitivity was firstly determined by analyzing the ring-down time variations of a gas mixture of 53 and 107 ppbv NO_2 in synthetic air, as this reflects the expected background conditions of in situ measurements. Secondly, the eCL of HO_2 and CH_3O_2 of the PeRCEAS instrument were experimentally determined for an inlet pressure of 300 hPa by generating a set of known HO_2 and 50 % HO_2/50 % CH_3O_2 volume mixing ratios. The HO_2 effective chain length is then determined by $eCL = \Delta x_{NO_2}/x_{HO_2}$, and the CH_3O_2 chain length is deduced from the chain length calibration of the 50 %/50 % radical mixture. The peroxy radical detection limit can then be calculated by dividing the NO_2 detection limit by the eCL.

3.1 NO_2 detection limit

To assess the detection limit of the NO_2 optical detector, a reference measurement of two different NO_2 volume mixing ratios in synthetic air over the expected range of ambient ozone concentrations was analyzed. The NO_2/synthetic air mixture was provided to the inlet cone, and a flow of 1 sLpm was drawn by the detectors. The inlet chamber pressure was kept constant at 300 hPa. Figure 8 shows exemplary 1 s averages of the ring-down times recorded from one detector.

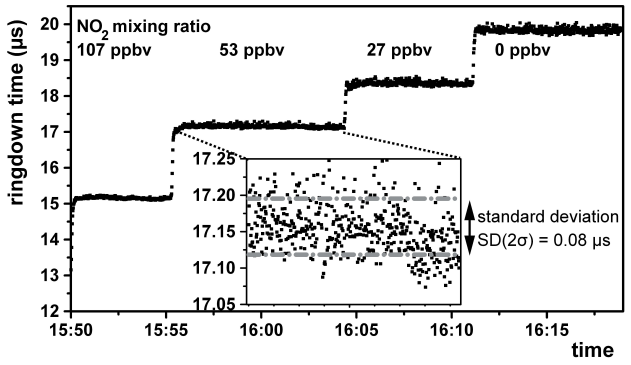

Fig. 8. Ring-down measurement of different NO_2 volume mixing ratios in synthetic air.

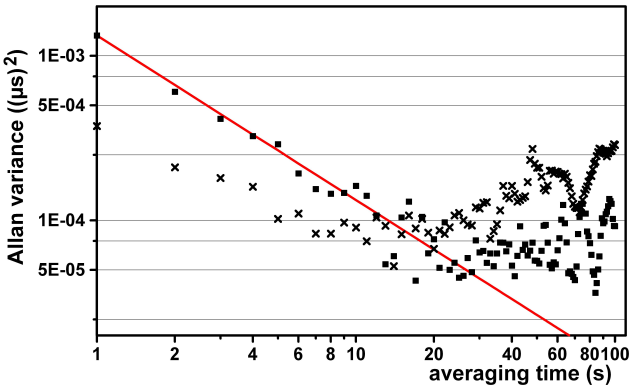

Fig. 9. Allan variance of the 53 ppbv NO_2 (black dots) and the 107 ppbv NO_2 (black crosses) in synthetic air measurement as depicted in Fig. 8. The red line corresponds to the black dots and indicates a slope of −1.0, which is expected for white noise only.

The measurement yields a value of the absorption cross section of $\sigma_{NO_2}^{408.9nm} = 6.5 \times 10^{-19}$ cm^2 molecule^{-1} with a relative error of ±2 % at the laser wavelength of 408.9 nm, a temperature of 296 K and a pressure of 300 hPa, in very good agreement with measurements of Vandaele et al. (2002) and Nizkorodov et al. (2004). The cited profiles may be used without requiring a convolution with the laser linewidth of 1 MHz ∼ 6×10^{-4} pm or the laser wavelength scanning range of 10 GHz ∼ 5 pm as both values are small compared to the cross-section profile structures.

The 1σ standard deviation for the ring-down time of both the 53 ppbv and 107 ppbv NO_2 measurement is below 0.04 µs, corresponding to a minimum detection limit of the absorption coefficient of 4.6×10^{-9} cm^{-1} $(\sqrt{\text{Hz}})^{-1}$ or a volume mixing ratio of 1 ppbv $(\sqrt{\text{Hz}})^{-1}$ at an inlet pressure of $p = 300$ hPa and a temperature of $T = 296$ K.

Figure 9 shows the corresponding Allan variances (Allan, 1966), indicating an optimum averaging time of ∼ 40 s for the 53 ppbv mixture with a minimum (1σ) detectable mixing ratio of 0.3 ppbv (or a concentration of 2×10^9 molecules cm^{-3}). Longer averaging times are influenced by slow temperature drifts affecting both the laser and the resonator characteristics. For peroxy radical measurements the duration of a background and amplification mode is set to 60 s to additionally allow the gas flow to settle about 15 s. The NO_2 detector sensitivity was tested for different concentrations of H_2O, CO and NO, and no significant variation was observed. The present NO_2 detection limit is adequate for the peroxy radical measurement task, but is limited by the characteristics of the laser source used. Different types of broadband diode lasers without extended cavities are at the moment investigated as possible improvements. Initial laboratory characterizations using a similar V-resonator show promising results in the form of decreased ring-down time noise.

3.2 Effective chain length calibration

The effective chain lengths of the PeRCEAS instrument were calibrated using a peroxy radical source introduced by Schultz et al. (1995); the employed model resembling the one characterized by Stöbener (1999), and described in detail by Reichert et al. (2003). Briefly, synthetic air is enriched with a known amount of water, flown through a quartz glass tube and provided to the PeRCEAS inlet. Shortly before being sucked in, the air is illuminated by a Hg/Ne gas UV lamp (type Pen-Ray, LOT-QuantumDesign GmbH), thus water is photolysed and HO_2 is produced by the reaction of hydrogen with oxygen. A photomultiplier tube (PMT, type 1259 with a MgF_2 window; Hamamatsu Photonics) measures a portion of the transmitted intensity afterwards. Addition of 0.1 % vol CO assures the complete conversion to HO_2 by reacting with both the hydroxyl radical and oxygen. Addition of 1.6 % vol CH_4 instead produces a 50 %/50 % mixture of HO_2 and CH_3O_2.

For the pure HO_2 configuration, its concentration can be calculated using

$$[HO_2] = \frac{\sigma_{H_2O}^{184.9nm}}{\sigma_{O_2}^{184.9nm}} \times \frac{[H_2O]}{[O_2]} \times [O_3], \quad (6)$$

where $\sigma_{H_2O}^{184.9\,nm} = (7.14 \pm 0.10) \times 10^{-20}$ cm^2 molecule^{-1} is the absorption cross section of H_2O at 184.9 nm (Cantrell et al., 1997; the denoted error represents the ±1σ standard deviation), and $\sigma_{O_2}^{184.9nm} = (1.60 \pm 0.08) \times 10^{-20}$ cm^2 molecule^{-1} is the effective absorption cross section of O_2, which has been determined specifically for the radical source employed here according to Hofzumahaus et al. (1997); the denoted error represents the ±1σ standard deviation (Kartal, 2009). $[H_2O]$ is calculated from measurements of a dew point sensor (type DMP 248, Vaisala GmbH). $[O_2]$ is given by

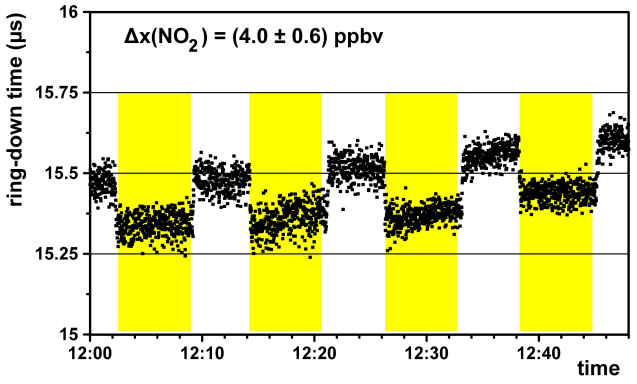

Fig. 10. Measurement of the maximum ozone concentration generated by the radical source. Periods with UV light entering the source are marked in yellow.

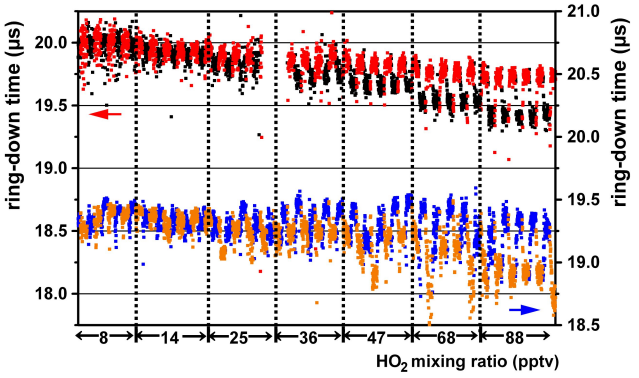

Fig. 11. eCL_{HO_2} calibration measurement at an inlet pressure of 300 hPa. Left *y* axis: reactor 1, red – background, black – amplification mode measurement. Right *y* axis: reactor 2, blue – background, orange – amplification mode measurement. The duration of each HO_2 volume mixing ratio measurement was 10 min.

the specifications of the used synthetic air gas cylinder (type Alphagaz, Air Liquide Deutschland GmbH).

To generate a range of different HO_2 or CH_3O_2 concentrations, pure N_2O gas is used as an optical filter (Cantrell et al., 1997) and absorbs part of the UV light reaching the photolysis zone. The measured PMT signal I is used as an $[O_3]$ proxy (Reichert et al., 2003):

$$\frac{[O_3]}{[O_3^{max}]} = \frac{I}{I_{max}}. \quad (7)$$

The maximum ozone concentration ($[O_3^{max}]$) generated by the radical source was measured in the PeRCEAS NO_2 detector while adding 0.01 sLpm of 600 ppmv NO in N_2 to the reactor to convert the ozone to NO_2. The UV light was modulated by means of a mechanical shutter every 7 minutes for a 5-minute background measurement. Figure 10 shows a measurement at an inlet pressure of 300 hPa which lasted 45 min. The ring-down time differences yield $x(O_3^{max}) = (4.0 \pm 0.6)$ ppbv, which together with the PMT measurement $I_{max} = 3.54$ V results in $x(O_3^{max})/I_{max} \sim (1.13 \pm 0.17)$ ppbv V^{-1}. This ratio is in reasonable agreement with a value of (1.06 ± 0.03) ppbv V^{-1} determined with a luminol chemiluminescence detector.

For the radical source used in this experiment, the mixing ratios are $x(O_3^{max}) \sim 4$ ppbv, $x(H_2O) \sim 2000$ ppmv, and $x(O_2) \sim 20$ % vol, thus $x(HO_2^{max}) \sim 200$ pptv.

The 1σ relative uncertainty of the HO_2 concentration amounts to ± 17 %, and consists of the uncertainties for the absorption cross sections of H_2O (1.5 %) and O_2 (5 %), for the H_2O concentration (5 %, from the dew point temperature accuracy of ± 2 K), and for the O_3 concentration (15 %). The O_2 concentration uncertainty is negligible. As was already briefly mentioned in the introduction, the relative uncertainty of the NO_2 volume mixing ratio is ± 2 %. Thus, the 1σ relative uncertainty of the eCL calculation is ± 19 %.

Multiple eCL calibrations for both HO_2 and a 50 %/50 % mixture of HO_2 and CH_3O_2 have been carried out for both PeRCEAS reactors at different pressure conditions. For this, the radical source stepwise produced HO_2 mixing ratios of (10–120) pptv for 10 minutes each, while the PeRCEAS reactors alternate between background and amplification mode every minute. An example of such a measurement at an inlet pressure of 300 hPa can be seen in Fig. 11, while Fig. 12 shows a transition process in detail. The switching of the solenoid valves induces a pressure pulse, and it takes about 15 s for the gas flow to stabilize itself afterwards. A part of this settling time is caused by the retention time of the sample air inside the reactor (2 s), the tube connecting the inlet and NO_2 detector (< 1 s) and the detector itself (5 s).

The resulting eCL determination is shown in Fig. 13. The ΔNO_2 values were calculated from the averages of both the background and the amplification mode ring-down times for a constant HO_2 volume mixing ratio. In this measurement the effective chain lengths for the two reactors are $eCL_{HO_2} = 82 \pm 17$ for reactor 1 and $eCL_{HO_2} = 103 \pm 21$ for reactor 2 (1σ uncertainty of 19 % as calculated above).

A total of 11 such calibrations were carried out over multiple days to test their reproducibility. The average effective chain lengths for the two reactors present in PeRCEAS are $eCL_{HO_2} = 88 \pm 17$ for reactor 1 and $eCL_{HO_2} = 110 \pm 21$ for reactor 2 (1σ uncertainty of 19 % as calculated above). The (statistical) 1σ standard deviations of the effective chain lengths of 10 and 9 are well below this uncertainty.

The dissimilar effective chain lengths of both reactors are most probably caused by small differences in their fabrication. Previous studies using luminol NO_2 detectors and adding 3 ppmv of NO to the reactors showed effective chain lengths of 79 ± 9 and 100 ± 13 (Chrobry, 2013). Lower eCL values are expected for these conditions as a NO mixing ratio of around 5 ppmv is expected to yield a maximum eCL.

The HO_2/CH_3O_2 mixture yielded effective chain lengths of $eCL_{mix} = 76 \pm 14$ for reactor 1 and $eCL_{mix} = 96 \pm 18$ for

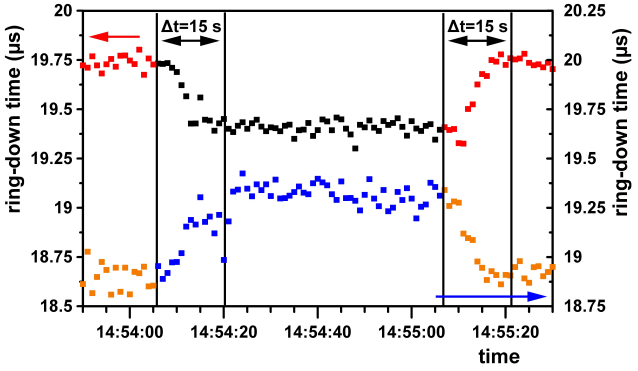

Fig. 12. Switching between background (reactor 1: left *y* axis, red; reactor 2: right *y* axis, blue) and amplification mode (reactor 1: left *y* axis, black; reactor 2: right *y* axis, orange); the two solid lines indicate a time difference of 15 s required for the gas flow stabilization.

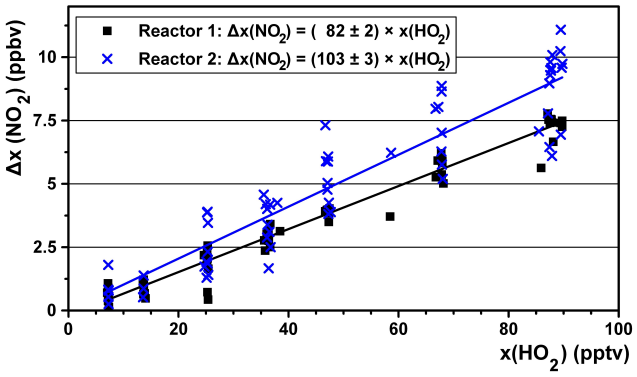

Fig. 13. Effective chain length determination corresponding to the calibration measurement shown in Fig. 11. Shown are the ΔNO_2 vs. HO_2 mixing ratios measured for both PeRCEAS reactors. The slopes of the linear fits represent their eCL.

reactor 2, which leads to effective chain lengths for CH_3O_2 of $eCL_{CH_3O_2} = 64 \pm 18$ for reactor 1 and $eCL_{CH_3O_2} = 82 \pm 23$ for reactor 2. As noted before in the introduction, the smaller effective chain length compared to eCL_{HO_2} is expected due to additional loss reactions, for example, the direct reaction of CH_3O with NO. The 1σ uncertainty is enhanced by a factor of $\sqrt{2}$ due to the difference being taken of two effective chain length calibrations.

For an inlet pressure of 200 hPa effective chain lengths of 55 ± 10 were determined, without significant difference between both reactors. Possible reasons for the effective chain length decrease include higher radical surface losses due to more turbulent flow conditions, a lower radical conversion efficiency due to smaller reactor retention times, and the pressure dependence of contributing reactions (e.g., Reaction R2).

The PeRCEAS instrument reported by Liu et al. (2009) differs both in scope (airborne measurements for PeRCEAS vs. ground-based measurements) and general layout (pressure stabilized inlet of PeRCEAS vs. Teflon tubing inlet, compact 19″ NO_2 detector with a diode laser for PeRCEAS vs. more voluminous Nd-YAG pumped dye laser setup). Its chain length is reported to be 150 ± 50 for standard pressure. Both instruments show peroxy radical (1σ) detection limits of ~ 3 pptv, albeit at different averaging times (120 s for PeRCEAS instead of 60 s), and at different inlet pressures (300 hPa for PeRCEAS instead of ~ 1000 hPa).

4 Summary and conclusion

The development and characterization of a peroxy radical chemical amplification instrument for airborne measurements with a CRDS NO_2 detector using optical feedback are reported. The ΔNO_2 detection by CRDS allows for the direct calculation of the RO_2^* volume mixing ratios without requiring a NO_2 calibration, and its sensitivity is free from interference of variations in the humidity and pressure levels. An optimum averaging time of 40 s yields a (1σ) minimum detectable NO_2 mixing ratio of 0.3 ppbv (resonator pressure 285 hPa).

For an inlet pressure of 300 hPa, the effective chain lengths of the reactors are $eCL_{HO_2} = 88 \pm 17$ for reactor 1 and $eCL_{HO_2} = 110 \pm 21$ for reactor 2. For CH_3O_2, the values are $eCL_{CH_3O_2} = 64 \pm 18$ for reactor 1 and $eCL_{CH_3O_2} = 82 \pm 23$ for reactor 2. These values lead to a (1σ) detection limit for the total sum of peroxy radicals RO_2^* between 3 and 5 pptv for an averaging time of 120 s (one background mode and one amplification mode measurement). For an inlet pressure of 200 hPa effective chain lengths for HO_2 of 55 ± 10 were measured, and thus a (1σ) detection limit for HO_2 of ~ 6 pptv (averaging time of 120 s) was determined.

As shown, the PeRCEAS airborne instrument provides a means to accurately measure mixing ratios of peroxy radicals in the pptv range in altitudes of up to 13 km. It is currently certified for aircraft operation, and will take part in the OMO (oxidation mechanisms observations in the extratropical free troposphere) mission onboard the HALO aircraft, whose start is scheduled for end of 2014.

Acknowledgements. We are indebted to the university mechanical workshop, especially for crafting the V-resonators. We acknowledge funding for this study by the University of Bremen, the State of Bremen, and the HALO SPP 1294 (Atmospheric and Earth system research) grant from the DFG Deutsche Forschungsgemeinschaft, including salary funding for the first author.

Edited by: J. Stutz

References

Allan, D. W.: Statistics of atomic frequency standards, Proc. IEEE, 54, 221–230, 1966.

Andrés Hernández, M. D., Burkert, J., Reichert, L., Stöbener, D., Meyer-Arnek, J., and Burrows, J. P.: Marine boundary layer peroxy radical chemistry during the AEROSOLS99 campaign: measurements and analysis, J. Geophys. Res., 106, 20833–20846, 2001.

Andrés-Hernández, M. D., Stone, D., Brookes, D. M., Commane, R., Reeves, C. E., Huntrieser, H., Heard, D. E., Monks, P. S., Burrows, J. P., Schlager, H., Kartal, D., Evans, M. J., Floquet, C. F. A., Ingham, T., Methven, J., and Parker, A. E.: Peroxy radical partitioning during the AMMA radical intercomparison exercise, Atmos. Chem. Phys., 10, 10621–10638, doi:10.5194/acp-10-10621-2010, 2010.

Andrés-Hernández, M. D., Kartal, D., Crowley, J. N., Sinha, V., Regelin, E., Martínez-Harder, M., Nenakhov, V., Williams, J., Harder, H., Bozem, H., Song, W., Thieser, J., Tang, M. J., Hosaynali Beigi, Z., and Burrows, J. P.: Diel peroxy radicals in a semi-industrial coastal area: nighttime formation of free radicals, Atmos. Chem. Phys., 13, 5731–5749, doi:10.5194/acp-13-5731-2013, 2013.

Bell, C. L., van Helden, J. P. H., Blaikie, T. P. J., Hancock, G., van Leeuwen, N. J., Peverall, R., and Ritchie, G. A. D.: Noise-immune cavity-enhanced optical heterodyne detection of HO_2 in the near-infrared range, J. Phys. Chem. A, 116, 5090–5099, 2012.

Berden, G. and Engeln, R.: Cavity Ring-Down Spectroscopy: Techniques and Applications, John Wiley & Sons Ltd, The Atrium, Southern Gate, Chichester, West Sussex, UK, doi:10.1002/9781444308259.fmatter, 2010.

Burkert, J., Behmann, T., Andrés Hernández, M. D., Weissenmayer, M., Perner, D., and Burrows, J. P.: Measurements of peroxy radicals in a forested area in Portugal, Chemosphere, 3, 3327–3338, 2001a.

Burkert, J., Andrés Hernández, M. D., Stöbener, D., Burrows, J. P., Weissenmayer, M., and Kraus, A.: Peroxy radical and related trace gas measurement in the marine boundary layer above the Atlantic Ocean, J. Geophys. Res., 106, 5457–5477, 2001b.

Busch, K. W. and Busch, M. A.: Cavity-Ringdown Spectroscopy, American Chemical Society, ACS Copyright Office, Publications Division, Washington, D.C., doi:10.1021/bk-1999-0720, 1999.

Cantrell, C. A. and Stedman, D. H.: A possible technique for the measurement of atmospheric peroxy radicals, Geophys. Res. Lett., 9, 846–849, 1982.

Cantrell, C. A., Stedman, D. H., and Wendel, G. J.: Measurement of atmospheric peroxy radicals by the chemical amplification, Anal. Chem., 56, 1496–1502, 1984.

Cantrell, C. A., Shetter, R. E., Lind, J. A., McDaniel, A. H., and Calvert, J.: An Improved Chemical Amplifier Technique for Peroxy Radical Measurements, J. Geophys. Res., 98, 2897–2909, 1993.

Cantrell, C. A., Zimmer, A., and Tyndall, G. S.: Absorption cross sections for water vapor from 183 to 193 nm, Geophys. Res. Lett., 24, 2195–2198, 1997.

Chrobry, A.: Development and laboratory characterization of a sampling system for airborne measurements of peroxy radicals using chemical amplification, Ph. D. dissertation, University of Bremen, Bremen, 2013.

Clemitshaw, K., Carpenter, L., Penkett, S., and Jenkin, M.: A calibrated peroxy radical chemical amplifier for ground-based tropospheric measurements, J. Geophys. Res., 102, 25405–25416, 1997.

Courtillot, I., Morville, J., Motto-Ros, V., and Romanini, D.: Sub-ppb NO_2 detection by optical feedback cavity-enhanced absorption spectroscopy with a blue diode laser, Appl. Phys. B, 85, 407–412, 2006.

Djehiche, M., Tomas, A., Fittschen, C., and Coddeville, P.: First cavity ring-down spectroscopy HO_2 measurements in a large photoreactor, Z. Phys. Chem., 225, 983–992, doi:10.1524/zpch.2011.0143, 2011.

Fleming, Z. L., Monks, P. S., Rickard, A. R., Heard, D. E., Bloss, W. J., Seakins, P. W., Still, T. J., Sommariva, R., Pilling, M. J., Morgan, R., Green, T. J., Brough, N., Mills, G. P., Penkett, S. A., Lewis, A. C., Lee, J. D., Saiz-Lopez, A., and Plane, J. M. C.: Peroxy radical chemistry and the control of ozone photochemistry at Mace Head, Ireland during the summer of 2002, Atmos. Chem. Phys., 6, 2193–2214, doi:10.5194/acp-6-2193-2006, 2006.

Fuchs, H., Brauers, T., Häseler, R., Holland, F., Mihelcic, D., Müsgen, P., Rohrer, F., Wegener, R., and Hofzumahaus, A.: Intercomparison of peroxy radical measurements obtained at atmospheric conditions by laser-induced fluorescence and electron spin resonance spectroscopy, Atmos. Meas. Tech., 2, 55–64, doi:10.5194/amt-2-55-2009, 2009.

Green, T. J., Reeves, C. E., Brough, N., Edwards, G. D., Monks, P. S., and Penkett, S. A.: Airborne measurements of peroxy radicals using the PERCA technique, J. Environ. Monitor., 5, 75–83, doi:10.1039/B204493E, 2002.

Hargrove, J., Wang, L., Muyskens, K., Muyskens, M., Medina, D., Zaide, S., Zhang, J.: Cavity ring-down spectroscopy of ambient NO_2 with quantification and elimination of interferences, Env. Sci. Technol., 40, 7868–7873, 2006.

Hastie, D. R., Weissenmayer, M., Burrows, J. P., and Harris, G. W.: Calibrated chemical amplifier for atmospheric RO_x measurements, Anal. Chem., 63, 2048–2057, 1991.

Heard, D.: Analytical Techniques for Atmospheric Measurement, Blackwell Publishing Ltd, Oxford, UK, 528 pp., doi:10.1002/9780470988510, 2006.

Hofzumahaus, A., Brauers, T., Aschmutat, U., Brandenburger, U., Dorn, H. P., Hausmann, M., Heßling, M., Holland, F., Plass-Dülmer, C., Sedlacek, M., Weber, M., and Ehhalt, D. H.: Reply, Geophys. Res. Lett., 24, 3039–3040, 1997.

Hofzumahaus, A., Rohrer, F., Lu, K., Bohn, B., Brauers, T., Chang, C.-C., Fuchs, H., Holland, F., Kita, K., Kondo, Y., Li, X., Lou, S., Shao, M., Zeng, L., Wahner, A., and Zhang, Y.: Amplified trace gas removal in the troposphere, Science, 324, 1702–1704, doi:10.1126/science.1164566, 2009.

Horstjann, M., Nenakhov, V., and Burrows, J. P.: Frequency stabilization of blue extended cavity diode lasers by external cavity optical feedback, Appl. Phys. B, 106, 261–266, 2012.

Kartal, D.: Characterization and optimization of a dual channel PERCA for the investigation of the chemistry of peroxy radicals in the upper troposphere, Ph. D. dissertation, University of Bremen, Bremen, 2009.

Kartal, D., Andrés-Hernández, M. D., Reichert, L., Schlager, H., and Burrows, J. P.: Technical Note: Characterisation of a DUALER instrument for the airborne measurement of peroxy radicals during AMMA 2006, Atmos. Chem. Phys., 10, 3047–3062, doi:10.5194/acp-10-3047-2010, 2010.

Lelieveld, J., Butler, T. M., Crowley, J. N., Dillon, T. J., Fischer, H., Ganzeveld, L., Harder, H., Lawrence, M. G., Martinez, M., Taraborrelli, D., and Williams, J.: Atmospheric oxidation capacity sustained by a tropical forest, Nature, 452, 737–740, 2008.

Liu, Y., Morales-Cueto, R., Hargrove, J., Medina, D., and Zhang, J.: Measurements of peroxy radicals using chemical amplification-cavity ringdown spectroscopy, Environ. Sci. Technol., 43, 7791–7796, 2009.

Maeda, Y., Aoki, K., and Munemori, M.: Chemiluminescence Method for the Determination of Nitrogen Dioxide, Anal. Chem., 52, 307–311, doi:10.1021/ac50052a022, 1980.

Mihelcic, D., Müsgen, P., and Ehhalt, D. H.: An improved method of measuring tropospheric NO_2 and RO_2 by matrix isolation and electron spin resonance, J. Atmos. Chem., 3, 341–361, 1985.

Monks, P.: Gas-phase radical chemistry in the troposphere, Chem. Soc. Rev., 34, 376–395, 2005.

Morville, J., Kassi, S., Chenevier, M., and Romanini, D.: Fast, low-noise, mode-by-mode, cavity-enhanced absorption spectroscopy by diode-laser self-locking, Appl. Phys. B, 80, 1027–1038, 2005.

Nizkorodov, S. A., Sander, S. P., and Brown, L. R.: Temperature dependence of high-resolution air-broadened absorption cross sections of NO_2 (415–525 nm), J. Phys. Chem. A, 108, 4864–4872, 2004.

O'Keefe, A. and Deacon, D. A. G.: Cavity ring-down optical spectrometer for absorption measurements using pulsed laser sources, Rev. Sci. Instrum., 59, 2544–2551, 1988.

Reichert, L., Andrés Hernández, M. D., Stöbener, D., Burkert, J., and Burrows, J. P.: Investigation of the effect of water complexes in the determination of peroxy radical ambient concentrations: implications for the atmosphere, J. Geophys. Res., 108, 4017, doi:10.1029/2002JD002152, 2003.

Sadanaga, Y., Matsumoto, J., Sakurai, K., Isozaki, R., Kato, S., Nomaguchi, T., Bandow, H., and Kajii, Y.: Development of a measurement system of peroxy radicals using a chemical amplification/laser-induced fluorescence technique, Rev. Sci. Instrum., 75, 864–872, 2004.

Schultz, M., Heitlinger, M., Mihelcic, D., and Volz-Thomas, A.: Calibration source for peroxy radicals with built-in actinometry using H_2O and O_2 photolysis at 185 nm, J. Geophys. Res. 100, 18811–18816, 1995.

Stöbener, D.: Weiterentwicklung einer Peroxyradikalquelle für die Kalibration von RO_2 – Messungen in Außenluft, Diploma thesis, University of Bremen, Bremen, 1999.

Thrush, B. A.: The chemistry of the stratosphere, Rep. Prog. Phys., 51, 1341–1371, 1988.

Vandaele, A. C., Hermans, C., Fally, S., Carleer, M., Colin, R., Mérienne, M.-F., Jenouvrier, A., and Coquart, B.: High-resolution Fourier transform measurement of the NO_2 visible and near-infrared absorption cross-section: temperature and pressure effects, J. Geophys. Res., 107, 4348, doi:10.1029/2001JD000971, 2002.

Wendisch, M. and Brenguier, J.-L.: In situ trace gas measurements, in: Airborne Measurements for Environmental Research: Methods and Instruments, Wiley-VCH, Berlin, 611 pp., 2013.

Whalley, L. K., Edwards, P. M., Furneaux, K. L., Goddard, A., Ingham, T., Evans, M. J., Stone, D., Hopkins, J. R., Jones, C. E., Karunaharan, A., Lee, J. D., Lewis, A. C., Monks, P. S., Moller, S. J., and Heard, D. E.: Quantifying the magnitude of a missing hydroxyl radical source in a tropical rainforest, Atmos. Chem. Phys., 11, 7223–7233, doi:10.5194/acp-11-7223-2011, 2011.

Appendix A

Table A1. Acronyms used in this paper.

Abbreviation	Meaning
(e)CL	(**e**ffective) **c**hain **l**ength
CIMS	**c**hemical **i**onization **m**ass **s**pectrometry
CRDS	**c**avity **r**ing-**d**own **s**pectroscopy
DUALER	**dual** channel chemical amplifi**er**
ECDL	**e**xtended **c**avity **d**iode **l**aser
HALO	**h**igh **a**ltitude and **lo**ng range research aircraft
LIF	**l**aser **i**nduced **f**luorescence
MIESR	**m**atrix **i**solation **e**lectron **s**pin **r**esonance
NICE-OHMS	**n**oise **i**mmune **c**avity **e**nhanced **o**ptical **h**eterodyne **m**olecular **s**pectroscopy
OF-CEAS	**o**ptical **f**eedback **c**avity **e**nhanced **a**bsorption **s**pectroscopy
OMO	**o**xidation **m**echanisms, **o**bservations in the extra-tropical free troposphere
PeRCA	**pe**roxy **r**adical **c**hemical **a**mplification
PeRCEAS	**pe**roxy **r**adical **c**hemical **e**nhancement and **a**bsorption **s**pectroscopy
PMT	**p**hoto**m**ultiplier **t**ube
PFA	**p**er**f**luor**a**lkoxy
PAN	**p**eroxy**a**cetyl **n**itrate
pptv, ppbv, ppmv	**p**arts **p**er **t**rillion/**b**illion/**m**illion of **v**olume
roc	**r**adius **o**f **c**urvature
sLpm	**s**tandard (p_{st} = 1013 hPa, T_{st} = 273.15 K) **l**itres **p**er **m**inute